# Jason-2 GDR
# Quality Assessment Report

# Cycle 121

## *14-10-2011 / 24-10-2011*

| Prepared by : | S. Philipps, CLS | |
| --- | --- | --- |
| | M. Ablain, CLS | |
| | P. Thibaut, CLS | |
| Accepted by : | DT/AQM, CLS | |
| Approved by : | E. Bronner, CNES | |

# 1.  Introduction

## 1.1.  Document overview

The purpose of this document is to report the major features of the data quality from the Jason-2 mission. The document is associated with data dissemination on a cycle per cycle basis.
This document reports results from Jason-2 GDRs.

The objectives of this document are :

> To provide a data quality assessment
> To provide users with necessary information for data processing
> To report any change likely to impact data quality at any level, from instrument status to software configuration
> To present the major useful results for the current cycle

## 1.2.  Software version

This cycle has been produced with the Processing Software V3-1p1p2. The results presented in this report have been performed with GDR products in version T. A detailed description of the products can be found in the Jason-2 user handbook ([2]) and the GDR version T product disclaimer ([1]).
Note that for this cycle there was an AMR recalibration for 18.7GHz channel and for 34.0 GHz channel (Arcs system).

## 1.3.  Cycle quality and performances

Data quality for this cycle is nominal.
Analysis of crossovers and sea surface variability indicate that system performances are close to usual values that are obtained from TOPEX/POSEIDON or Jason-1 data. For this cycle, the crossover standard deviation is 7.18 cm rms. When using a selection to remove shallow waters (1000 m), areas of high ocean variability and high latitudes ($> |50|$ deg.) it decreases down to 5.03 cm rms.
The standard deviation of Sea Level Anomalies (SLA) relative to a 7-year mean (based on T/P data) is 11.64 cm. When using a selection to remove shallow waters (1000 m), areas of high ocean variability and high latitudes ($> |50|$ deg) it lowers to 9.98 cm .

- Performances from crossover differences are detailed in the dedicated **section Crossover statistics**.
- Detailed CALVAL results are presented in **section 3**.

## 1.4.  Information about tracking mode

Jason-2 is able to track data with several onboard tracker algorithms : SGT, Median and Diode/DEM. SGT is the same tracker as the one used for Jason-1. It was only used during the very first days of Jason-2. Median mode is similar to the one used by Envisat. Finally, Diode/DEM mode is a new technique using information coming from Diode and a digital elevation model available onboard. For more information about the different onboard tracker algorithms see [5].
During this cycle, Jason-2 used median mode.

## 2. Data coverage and edited measurements

This section presents results that illustrate data quality during this cycle. These verification products are produced operationally so that they allow long term monitoring of missing and edited measurements.

### 2.1. Missing measurements

This cycle has no missing pass. Missing measurements relative to a nominal ground track are plotted on figure 1.

The map below illustrates missing 1Hz measurements in the GDRs, with respect to a 1 Hz sampling of a nominal repeat track. Missing measurements occur over land, especially regions with high relief. This is normal for use of median tracking mode.
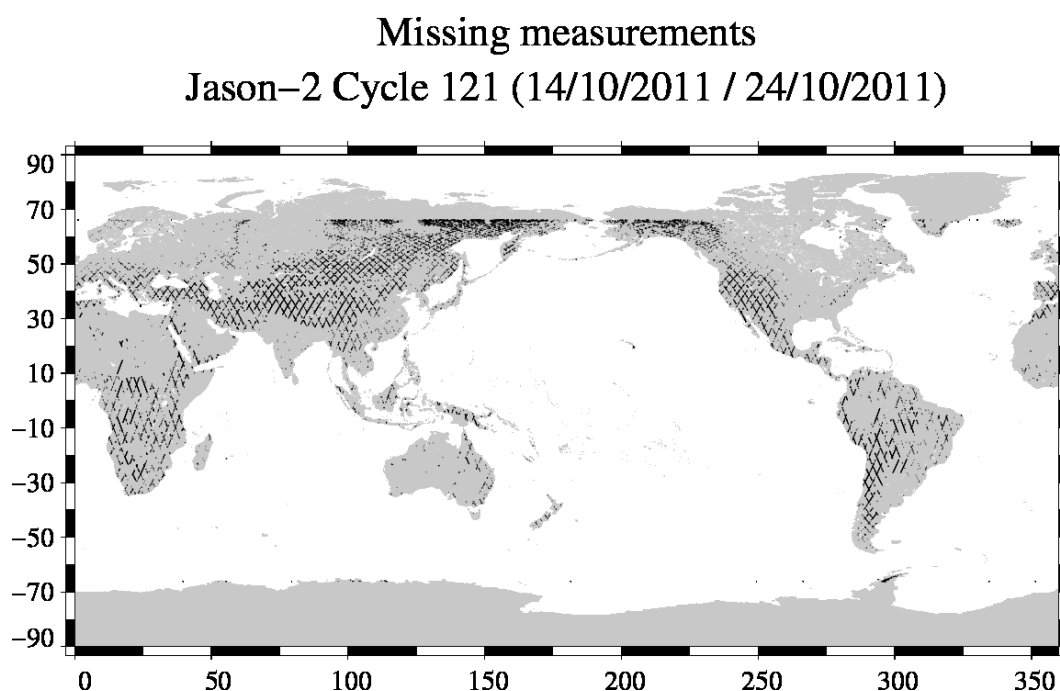
Missing measurements
Jason–2 Cycle 121 (14/10/2011 / 24/10/2011)



FIG. 1 – *Missing measurements for cycle 121.*

## 2.2.  Edited measurements

Editing criteria are defined for the GDR product in Jason-2 User Handbook [2].

The editing criteria are defined as minimum and maximum thresholds for various parameters. Measurements are edited if at least one parameter does not lie within those thresholds. These thresholds are expected to remain constant throughout the Jason-2 mission, so that monitoring the number of edited measurements allows a survey of data quality.

In the following, only measurements over ocean are kept. This is done by applying an ocean-land mask, instead of using the surface type information available in the products (surface_type, rad_surf_type). There is no impact on global performance estimations since the more significant results are derived from analyses in open ocean areas.

The rain flag is not used for data selection.

The number and percentage of points removed by each criterion is given on the following table. Note that these statistics are obtained with measurements already edited for ice flag (12.37 % of points removed).

| Parameters | Min threshold | Max threshold | Unit | Nb removed | % removed | % mean removed |
|---|---|---|---|---|---|---|
| Sea surface height | -130.000 | 100.000 | $m$ | 1608 | 0.31 | 0.27 |
| Sea level anomaly | -2.000 | 2.000 | $m$ | 2968 | 0.57 | 0.55 |
| Nb measurements of range | 10.000 | _ | _ | 2194 | 0.42 | 0.36 |
| Std. deviation of range | 0.000 | 0.200 | $m$ | 7370 | 1.41 | 1.38 |
| Square off nadir angle | -0.200 | 0.640 | $deg^2$ | 4292 | 0.82 | 0.77 |
| Dry tropospheric correction | -2.500 | -1.900 | $m$ | 0 | 0.00 | 0.00 |
| Combined atmospheric correction | -2.000 | 2.000 | $m$ | 0 | 0.00 | 0.00 |
| AMR wet tropospheric correction | -0.500 | -0.001 | $m$ | 312 | 0.06 | 0.08 |
| Ionospheric correction | -0.400 | 0.040 | $m$ | 4728 | 0.91 | 1.00 |
| Significant wave height | 0.000 | 11.000 | $m$ | 2211 | 0.42 | 0.44 |
| Sea State Bias | -0.500 | 0.000 | $m$ | 1069 | 0.20 | 0.17 |
| Backscatter coefficient | 7.000 | 30.000 | $dB$ | 1446 | 0.28 | 0.30 |
| Nb measurements of sigma0 | 10.000 | _ | _ | 2156 | 0.41 | 0.36 |
| Std. deviation of sigma0 | 0.000 | 1.000 | $dB$ | 12507 | 2.40 | 2.27 |
| Ocean tide | -5.000 | 5.000 | $m$ | 470 | 0.09 | 0.07 |
| Equilibrium tide | -0.500 | 0.500 | $m$ | 0 | 0.00 | 0.00 |
| Earth tide | -1.000 | 1.000 | $m$ | 0 | 0.00 | 0.00 |
| Pole tide | -15.000 | 15.000 | $m$ | 0 | 0.00 | 0.00 |
| Altimeter wind speed | 0.000 | 30.000 | $m.s^-$ | 3547 | 0.68 | 0.66 |
| Global statistics of edited measurements by thresholds | _ | _ | _ | 18593 | 3.56 | 3.42 |

TAB. 1: *Table of parameters used for editing.*

The measurements rejected during the editing process are shown in figure 2. They are mainly situated in ice regions and in regions with disturbed sea state.
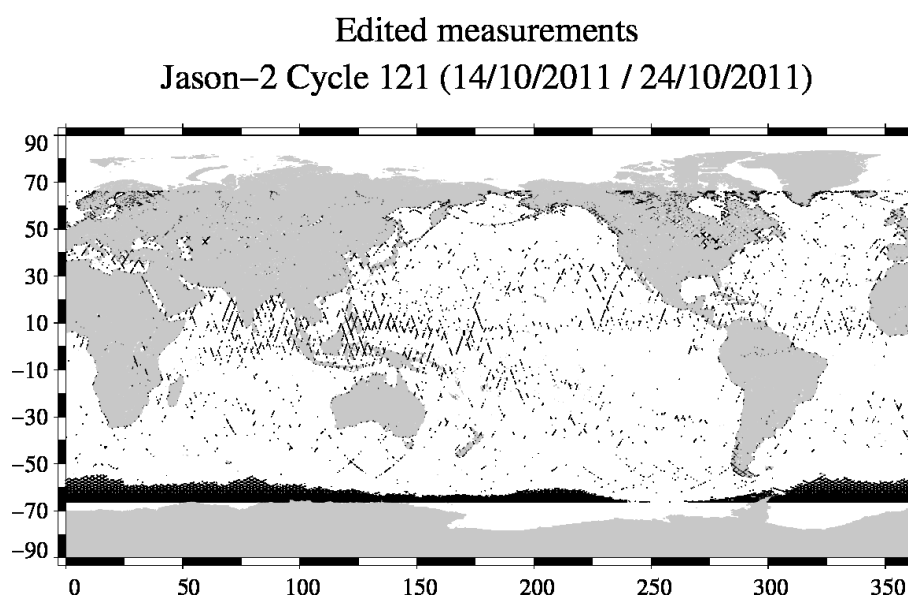
Edited measurements
Jason−2 Cycle 121 (14/10/2011 / 24/10/2011)



FIG. 2 – *Edited measurements for cycle 121.*

Map in figure 3 shows the percentage of valid measurements by sample. Wet zones or zones with sea ice appear in the plot as regions with less valid data, as it was also the case for Topex, Poseidon-1, and Jason-1 altimeters : measurements may be corrupted by rain or sea ice. They were therefore removed by editing. Compared with the usual maps obtained for Topex and Jason-1, there are less removed data in these zones and in the areas of strong sea states.

Jason−2 Cycle 121
14/10/2011 − 24/10/2011



Percentage of data valid
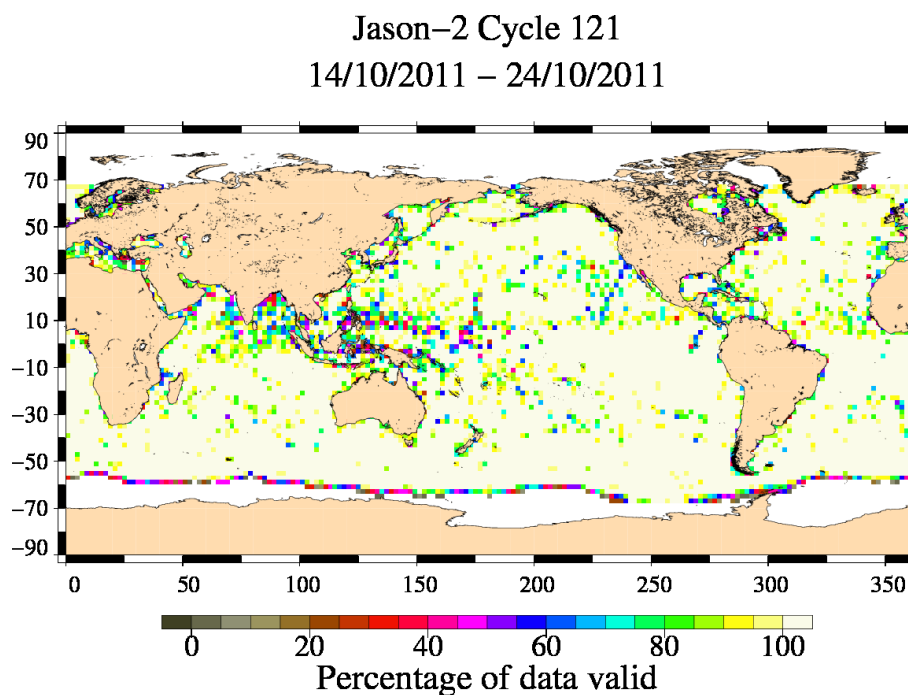
FIG. 3 – *Percentage of valid measurements for cycle 121.*

# 3. Instrumental and geophysical parameter analysis

Monitoring of instrumental and geophysical parameters is important in order to detect possible problems. When monitoring parameters over long periods, possible drifts or jumps can be detected. These verification products are produced operationally so that they allow systematic monitoring of the main relevant parameters. When possible, comparison with Jason-1 data are done.

## 3.1. Jason-2 altimeter and sensor

### 3.1.1. Sensor status

A detailed assessment of the Jason-2 sensor (Poseidon-3) is made in a separate bulletin to be made available on request ([8]).

### 3.1.2. Jason-2 altimeter status

This section presents the general status of the altimeter for main instrumental variations through the Jason-2 mission. Two calibration modes are used to monitor the altimeter internal drifts and compute the altimetric parameters. They are programmed about three times per day, over land.
The CAL1 mode measures the Point Target Response (PTR) of the altimeter in Ku and C bands. Among the parameters extracted from the PTR are :
  – the internal path delay
  – the total power of the PTR
The evolutions of these parameters as a function of time are plotted to monitor the ageing of the altimeter.
The CAL2 mode measures the low pass filter of the altimeter in Ku and C bands.
Notice that in the Jason-2 products, the range is corrected for the internal path delay and the backscatter coefficient takes into account the total power of the measured PTR.
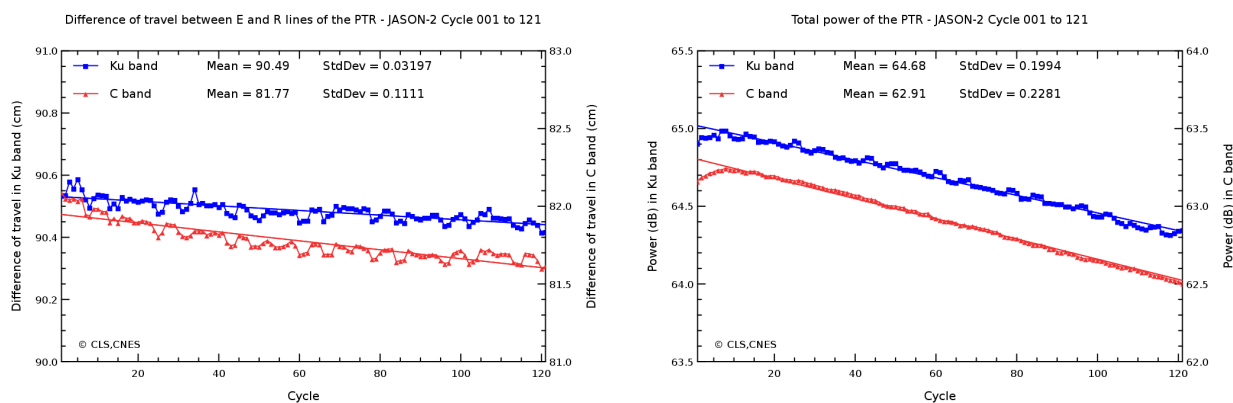


FIG. 4 – *Internal path delay (left) and total power of the PTR (right) for Ku- and C-band.*

## 3.2. Significant wave height

Figure 5 shows wave estimations derived from altimeter measurements. Therefore significant wave height data from the current cycle are averaged over a grid of 2° by 2° resolution and smoothed afterwards. Wave height may reach several meters.
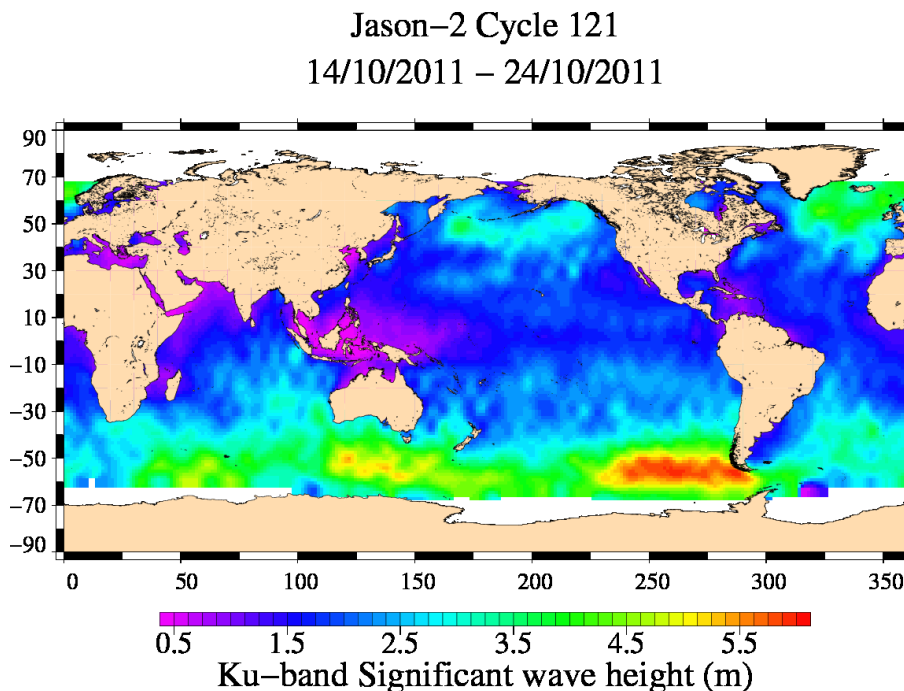
### Jason−2 Cycle 121
### 14/10/2011 − 24/10/2011



Ku−band Significant wave height (m)

FIG. 5 – *Significant wave height for cycle 121.*

The daily average of Ku-band SWH for Jason-1 and Jason-2 is plotted as a function of time on figure 6. They show similar features. Differences between SWH of both satellites - determined during Jason-2 verification phase - is 1.1 cm.
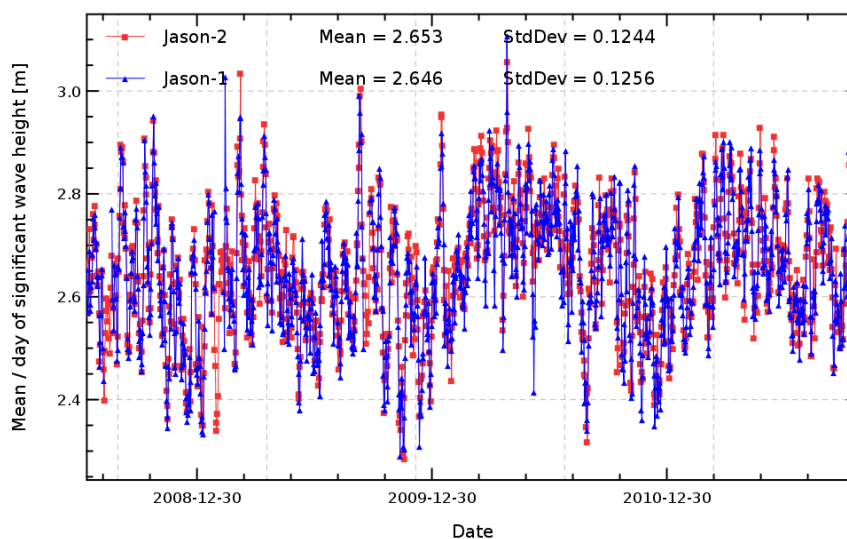


FIG. 6 – *Daily monitoring of Ku-band significant wave height for Jason-2 and Jason-1.*

## 3.3. Backscattering coefficient

The daily average of Ku-band backscattering coefficient for Jason-1 and Jason-2 is plotted as a function of time on figure 7. Beside a difference of about 0.14 dB (determined during the verification phase of Jason-2), they show similar features.
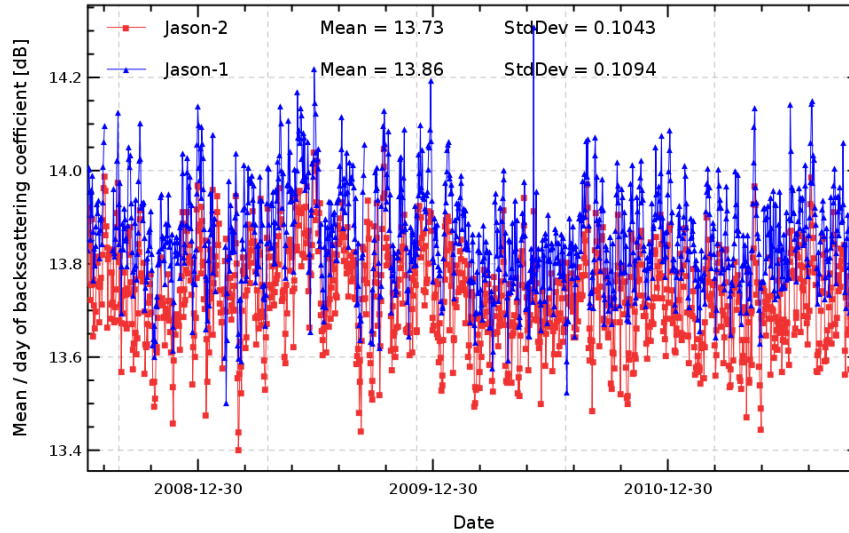


FIG. 7 – *Daily monitoring of Ku-band backscattering coefficient for Jason-2 and Jason-1.*

## 3.4. Dual frequency ionosphere correction

The daily average of dual-frequency ionosphere correction for Jason-1 and Jason-2 is plotted as a function of time on figure 8. They show similar features, but a bias of about 8.6 mm is visible. This bias comes from Ku and C-band range differences between Jason-1 and Jason-2. More information can be found in [6].
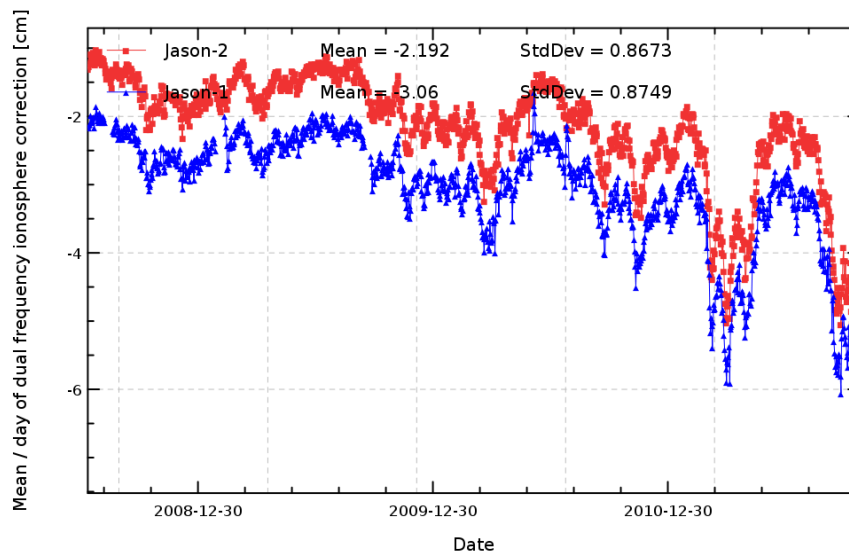


FIG. 8 – *Daily monitoring of dual-frequency ionosphere correction for Jason-2 and Jason-1.*

## 3.5. Altimeter wind speed

Figure 9 shows altimeter wind estimations derived from altimeter measurements. Therefore the data from the current cycle are averaged over a grid of 2° by 2° resolution and smoothed afterwards.
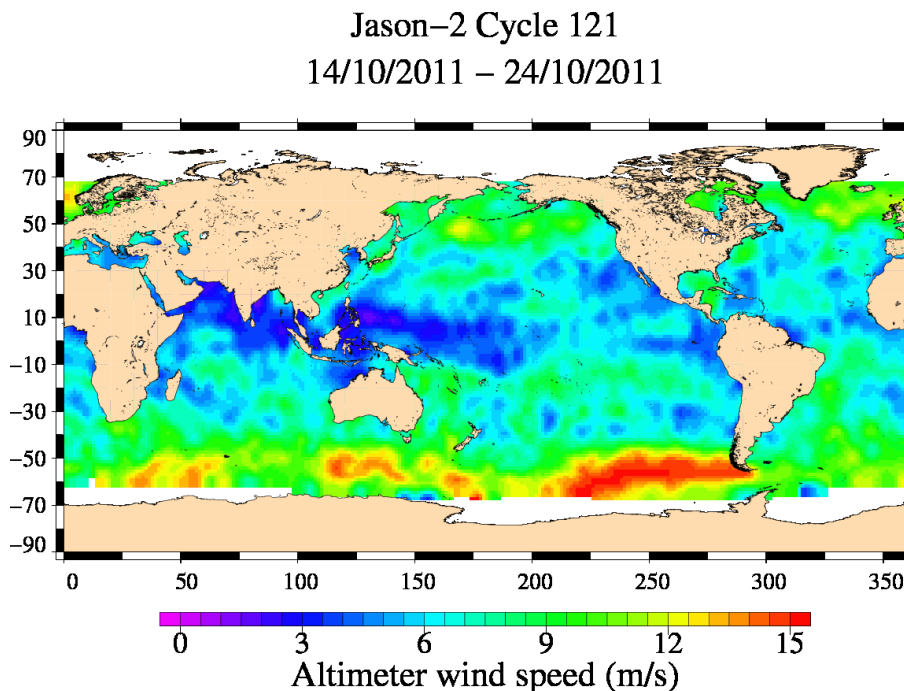


FIG. 9 – *Altimeter wind speed for cycle 121.*

The daily average of altimeter wind speed for Jason-1 and Jason-2 is plotted as a function of time on figure 10. They show similar features, but a bias of about 0.4 m/s is visible. This is inline with the observed bias of the backscattering coefficient.
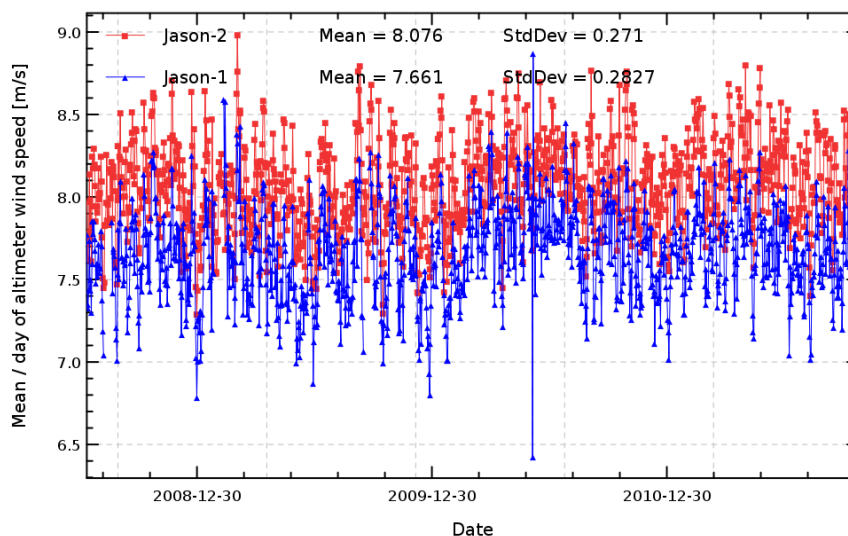


FIG. 10 – *Daily monitoring of altimeter wind speed for Jason-2 and Jason-1.*

## 3.6.  Radiometer parameters

The figure 11 shows the mean and standard deviation of wet troposphere correction (radiometer - ECMWF) difference by pass for current cycle.
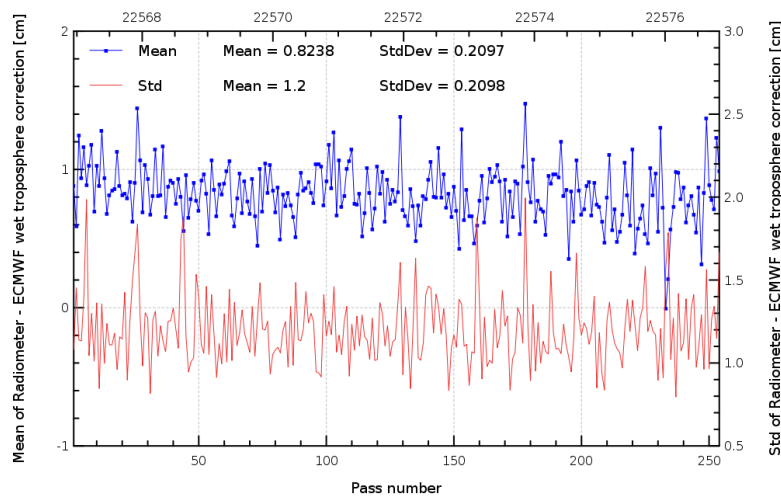


FIG. 11 – *Pass monitoring of wet troposphere differences between radiometer and ECMWF model for Jason-2 cycle 121.*

After a safehold mode of Jason-1, occured in August 2008, the JMR showed some thermal instability. Jason-1 radiometer (JMR) showed therefore daily differences up to 7 mm versus ECMWF model. Furthermore, the JMR is impacted by the yaw maneuvers, leading to differences of up to 2 or 3 mm. For Jason-2, an Autonomous Radiometer Calibration System (ARCS) is used prior to GDR production for the Jason-2 radiometer (AMR) in order to monitor calibrations and recalibrate if necessary (for more details see [4]). The plot of daily means of (Radiometer - ECMWF) wet troposphere correction was quite stable, even though ARCS does not use the ECMWF model to calibrate the AMR. Nevertheless small variations of up to 2 mm amplitude are observable. They can be due to (among others) evolution of ECMWF model or ARCS calibrations. Especially since mid-2011, the frequency of recalibrations has increased, as brightness temperatures of AMR are drifting and occasionnally show jumps. Though for GDR, these drifts and jumps are approximatively corrected by ARCS (by discrete values), drifts are still visible within a cycle. Furthermore, the application of a discrete recalibration can also lead to jumps in the time series.

The AMR calibration at the beginning of this cycle induces a jump of several mm in radiometer wet troposphere correction minus ECMWF model difference between end of cycle 120 and start of cycle 121 (see figure 13 : black vertical lines indicate application of new AMR antenna temperature coefficients for GDR data). During this cycle, the difference shows a small drift.
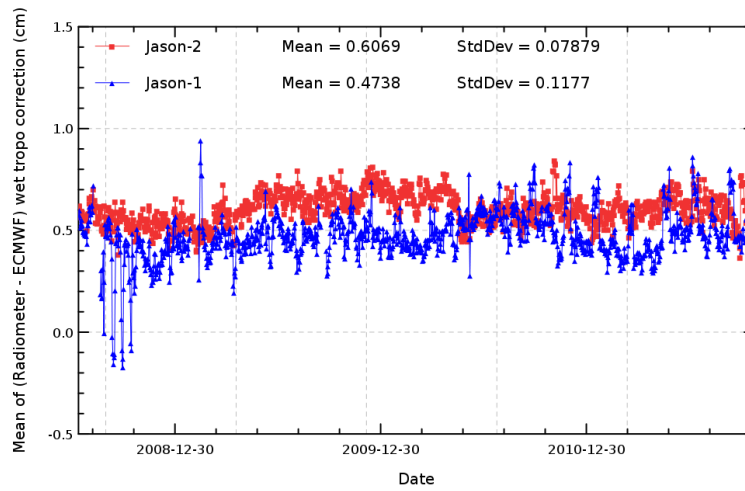
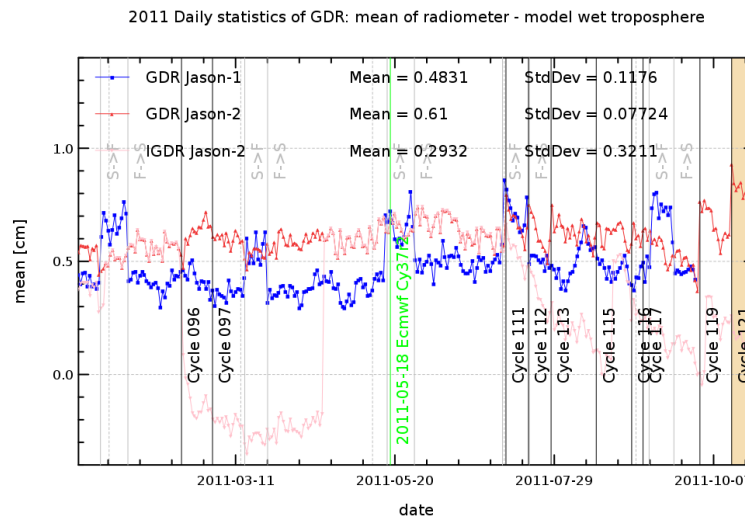FIG. 12 – *Daily monitoring of wet troposphere differences between radiometer and ECMWF model*



FIG. 13 – *Daily monitoring of wet troposphere differences between radiometer and ECMWF model for year 2011.*

# 4. Crossover Analysis

## 4.1. Overview

SSH crossover differences are the SSH differences between ascending and descending passes where they cross each other. Crossover differences are systematically analyzed to estimate data quality and the Sea Surface Height (SSH) performances. SSH crossover differences are computed from the valid data set on a one cycle basis, with a maximum time lag of 10 days, in order to limit the effects of ocean variability which are a source of error in the performance estimation. The mean SSH crossover differences should ideally be close to zero and standard deviation should ideally be small.

Nevertheless SLA varies also within 10 days, especially in high variablity areas. Furthermore, due to lower data availability (due to seasonal sea ice coverage), models of several geophysical corrections are less precise in high latitude. Therefore an additional geographical selection - removing shallow waters, areas of high ocean variability and high latitudes ($> |50|$ deg) - is applied for cyclic monitoring.

## 4.2. Maps of SSH crossover differences

After data editing, applying additional geographical selection and using the standard Jason-2 algorithms, the crossover standard deviation is about 5.03 cm rms.
The map of the mean differences at crossovers (4 by 4 degrees by bins) is plotted for the current cycle on left panel of figure 14, whereas the right panel shows the whole Jason-2 period. Some weak geographical correlated differences are visible with positives values in northern Atlantic and negatives values in southern Atlantic.
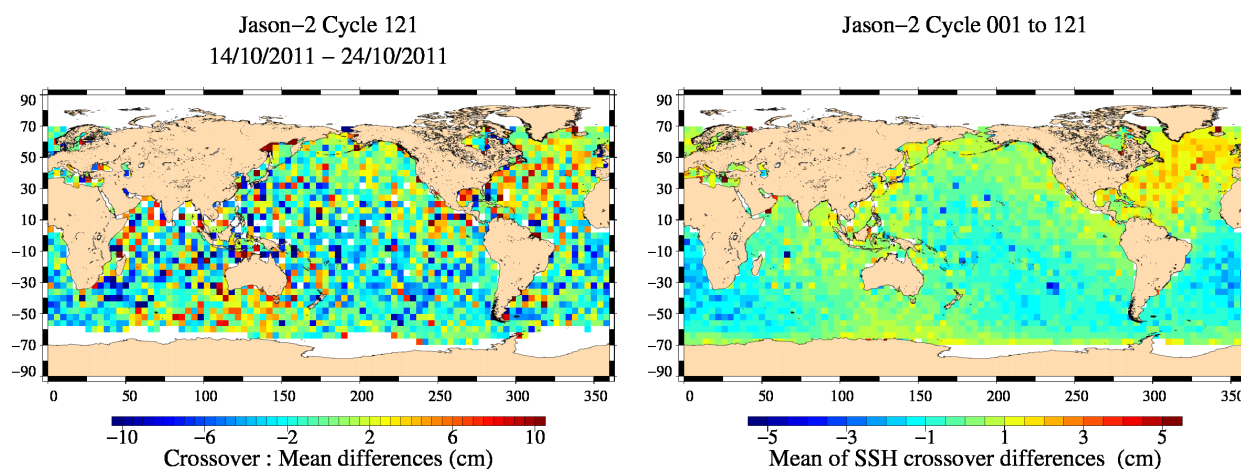


FIG. 14 – *Mean SSH at crossovers for cycle 121 (left) and over the whole Jason-2 period (right).*

## 4.3.   Cycle by cycle monitoring

The mean and standard deviation of SSH differences at crossovers are plotted for Jason-2 and Jason-1 as a function of time on a one cycle per cycle basis in figure 15. Note that cycle 001 of Jason-2 corresponds to cycle 240 of Jason-1. The statistics are computed after data editing and using the geographical selection criteria.

During the flight formation phase of Jason-2 (cycles 001 to 020), an intersection procedure is used to get homogeneous datasets on both missions. After Jason-1 was moved to its interleaved orbit, statistics are computed for each cycle based on Jason-2 cycle numbering. Data number may therefore vary between the missions (due to missing or edited measurements).  Jason-2 and Jason-1 show similar performances.
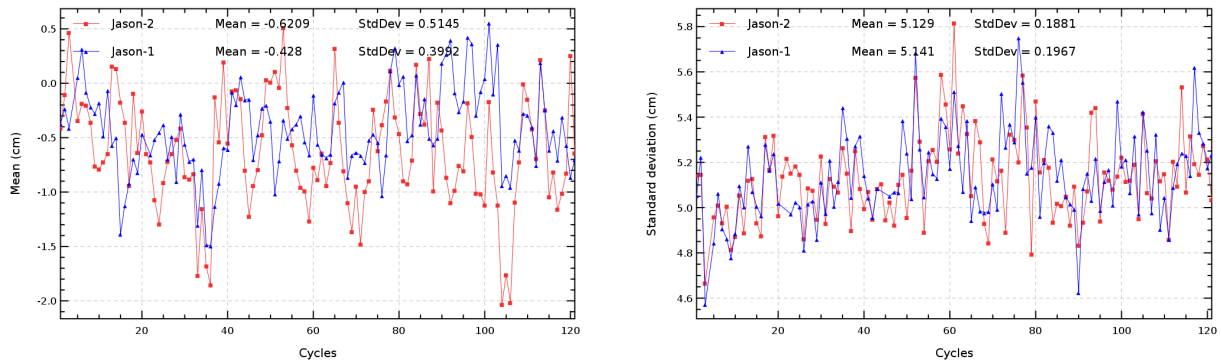


FIG. 15 – *Cyclic monitoring of mean (left) and standard deviation (right) of SSH differences at crossovers for Jason-1 and Jason-2.*

Figure 16 show the mean and the standard deviation of Jason-1 − Jason-2 10-day SSH crossovers. It does not show anomalies.
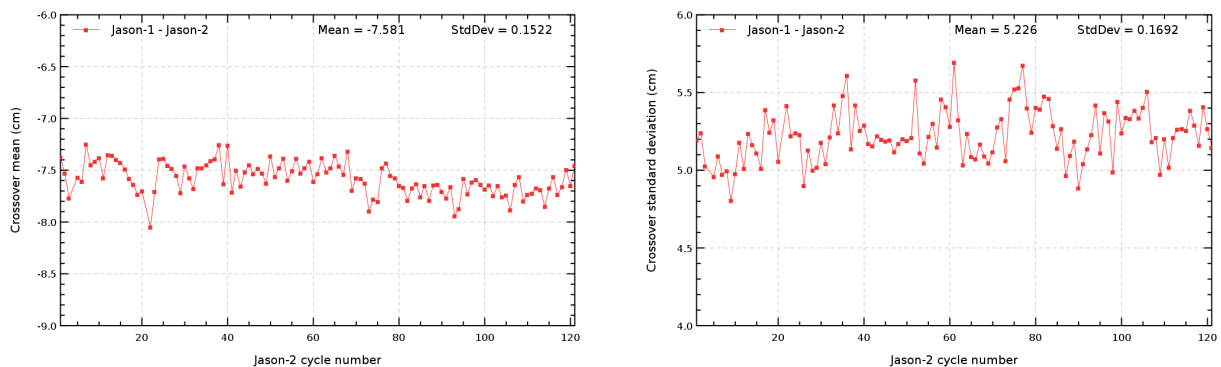


FIG. 16 – *Cyclic monitoring of mean (left) and standard deviation (right) of (Jason-1 − Jason-2) SSH differences at crossovers.*

## 4.4.  Comparison of pseudo time tag bias

The pseudo time tag bias is found by computing at SSH crossovers a regression between SSH and orbital altitude rate ($\dot{H}$), also called satellite radial speed :

$$SSH = \alpha\dot{H}$$

This method allows us to estimate the time tag bias but it absorbs also other errors correlated with $\dot{H}$ as for instance orbit errors. Therefore it is called "pseudo" time tag bias.

The monitoring of this coefficient estimated at each cycle is performed for Jason-1 and Jason-2 in the following figure. It highlights for both missions a bias close to -0.28 milliseconds with a 60-day signal. This weak pseudo time tag bias resulted in a small north/south bias on ascending/descending differences of Jason-1 SSH at crossover points lower than 0.5 cm.
For information, the Jason-1 pseudo time tag bias is taken into account in GDR-C product thanks to a new correction (pseudo_datation_bias_corr_ku).
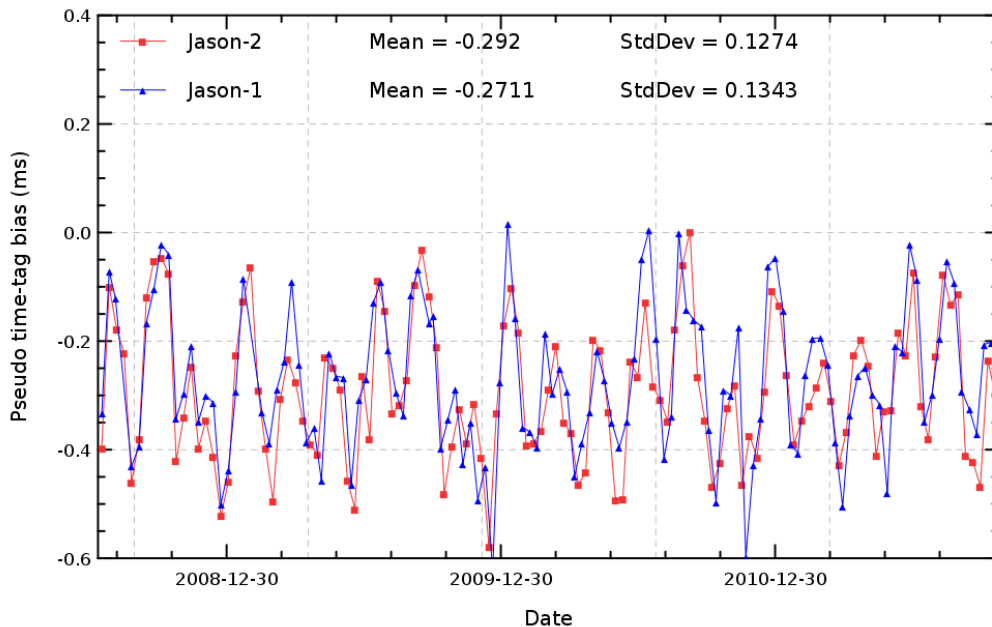


FIG. 17 – *Cyclic monitoring of pseudo time tag bias for Jason-1 and Jason-2.*

# 5. Along track analysis

## 5.1. Mean of along-track SLA

### 5.1.1. Temporal analysis

The monitoring of mean SLA for Jason-1 and Jason-2 (Figure 18 on left) and the monitoring of mean SLA diffrences between both missions (Figure 18 on right) show a very stable bias (close to 7.5 cm). This is mainly due to range differences and difference in dual-frequency ionosphere correction as explained in [6].

Note that during the Jason-2/Jason-1 flight formation phase (Cycles 1 to 20), the SSH bias estimation is performed very accurately (0.1 cm). This allows us to link together Jason-1 and Jason-2 MSL time data series (see section **Mean Sea Level estimations**).
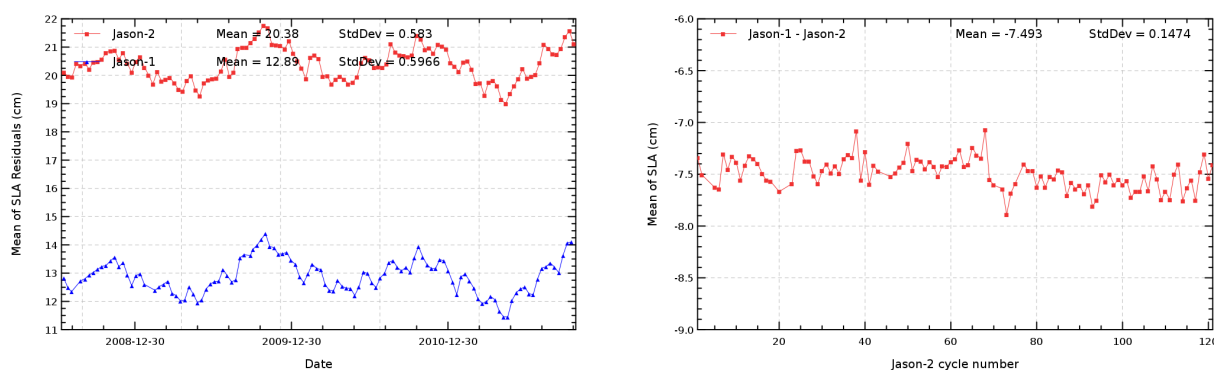


FIG. 18 – *Cyclic monitoring of mean SLA for Jason-1 and Jason-2 (left) and differences of (Jason-1 − Jason-2) mean SLA (right).*

### 5.1.2. Maps

Figures 19 and 20 respectively show the map of Jason-2 SLA relative to the MSS and differences higher than a 30 cm threshold (after centering the data). The latter figure shows that apart from isolated measurements that should be removed after refining the editing thresholds, higher differences are located in high ocean variability areas, as expected.

Since Jason-1 has moved to its new interleaved orbit, maps of direct Jason-1 − Jason-2 SLA measurements are no longer available. But differences of gridded SLA for Jason-1 and Jason-2 can be made. This difference is quite noisy for one cycle, especially as both satellites are shifted in time and sea state changes especially in regions of high ocean variablity. Therefore left panel of figure 21 shows an average over SLA grid differences from several cycles (since cycle 022). High variability regions as Gulf Stream and Antarctic circumpolar current are visible. On right panel of figure 21, colocated Jason-1 − Jason-2 SLA differences averaged over the period of flight formation phase (cycle 001 to 020) are shown. As both satellites measure the same oceanic features only 55 s apart, only a weak hemispheric bias is visible (likely due to differences in orbit processing).
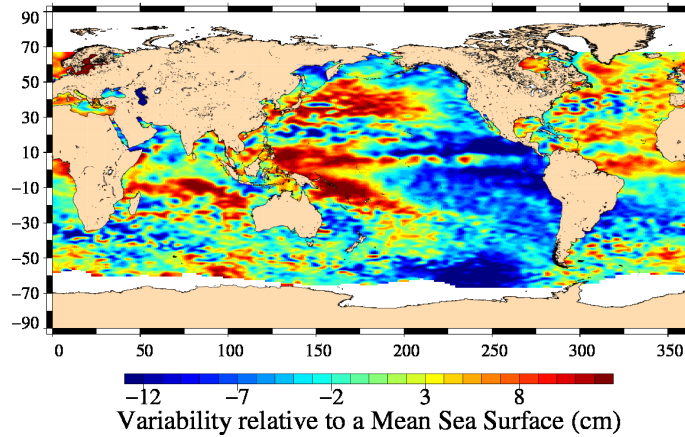
Jason−2 Cycle 121
14/10/2011 − 24/10/2011

Variability relative to a Mean Sea Surface (cm)

FIG. 19 – *Sea level anomaly relative to MSS for cycle 121.*



Valid data: (SSH − MSS) differences greater than 30 cm
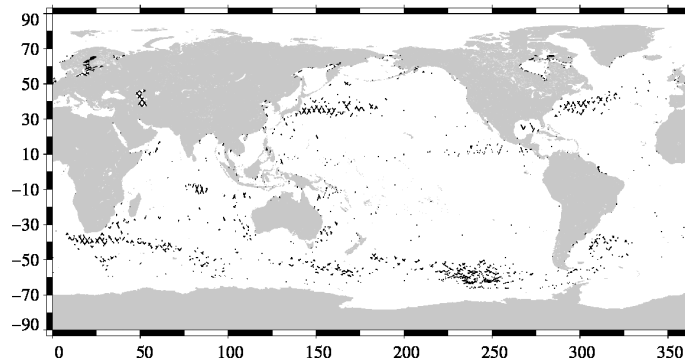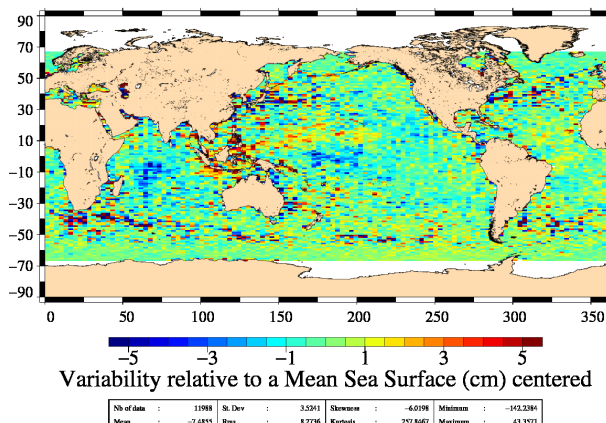Jason−2 Cycle 121 (14/10/2011 / 24/10/2011)

FIG. 20 – *Differences higher than a 30 cm threshold for cycle 121.*



Jason−1 − Jason−2 (Cycle 022 to 121)

Variability relative to a Mean Sea Surface (cm) centered

| Nb of data | : | 11988 | St. Dev | : | 3.5241 | Skewness | : | −6.0198 | Minimum | : | −142.2384 |
| Mean | : | −7.4855 | Rms | : | 8.2726 | Kurtosis | : | 257.8467 | Maximum | : | 43.3571 |



Differences of SLA before orbit error correction
Jason−1 − Jason−2 (Cycle 001 − 020)

Mean ( cm ), X−X

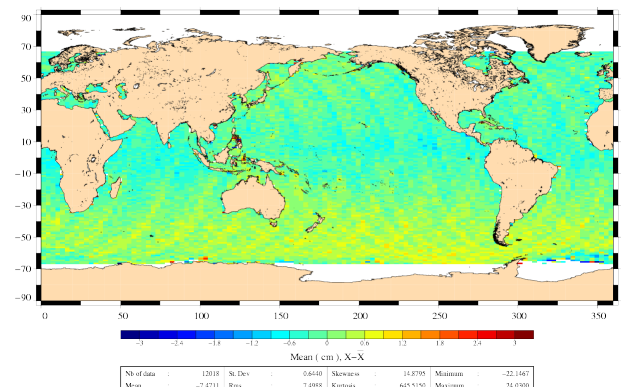| Nb of data | : | 12018 | St. Dev | : | 0.6440 | Skewness | : | 14.8795 | Minimum | : | −22.1467 |
| Mean | : | −7.4711 | Rms | : | 7.0988 | Kurtosis | : | 645.5150 | Maximum | : | 24.0300 |

FIG. 21 – *Jason-1 − Jason-2 SLA differences averaged over whole Jason-2 period since cycle 022 (left), and for flight formation phase (cycle 001 to 020) (right).*

## 5.2.  Along-track performances

Sea Level Anomaly (SLA) statistics are computed from repeat-track analysis. The plot below gives the standard deviation of the SLA for each cycle over the whole data set (shallow waters are excluded).
There are no values for Jason-1 during Jason-2 cycle 21 and half of cycle 22 (corresponding to Jason-1 cycles 260 and 261) because the Jason-1 satellite is moved to the Tandem Mission orbit on the new ground track spacing to the West of Jason-2. This was already the ground track of TOPEX during its Tandem Mission with Jason-1. In addition, Jason-1 is temporally shifted by 5 days.
A degradation of Jason-1 performance is observed after the orbit change, indeed the MSS (necessary for SLA computation) adds errors when used outside the nominal T/P / Jason-1 / Jason-2 ground track (Dorandeu et al., 2004 [7]).
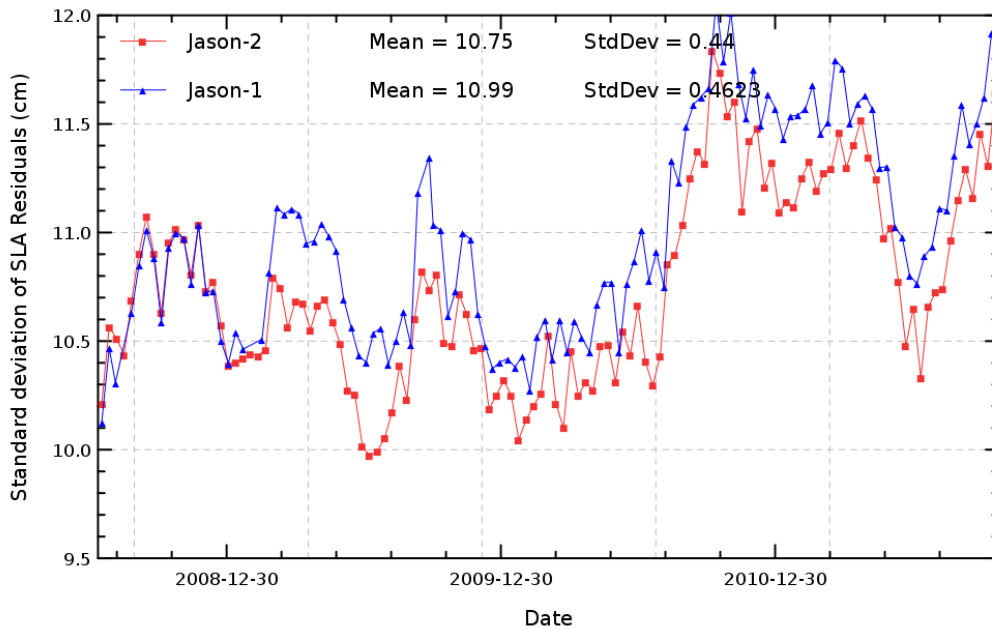


FIG. 22 – *Cyclic monitoring standard deviation of along track SLA for Jason-1 and Jason-2.*

# 6.  Mean Sea Level estimations (MSL)

## 6.1.  Global MSL trend

During the flight formation phase of Jason-2 (till cycle 020), both Jason satellites flew on the same ground track, only 55s apart. They therefore measured the same features, allowing to calibrate Jason-2. This allowed to link precisely the MSL time series of Jason-1 and Jason-2. The uncertainty of the bias value between the two time series is less than 1 mm. The evolution of the ocean mean sea level can therefore be precisely observed on a continual basis since 1993 thanks to the 3 reference missions : TOPEX/Poseidon, Jason-1 and now Jason-2.

Wet troposphere correction, inverse barometer correction, GIA (-0.3 mm/yr) are applied to calculate the MSL and the data series are linked together accurately thanks to the formation flying phases. The following global bias are applied : 8.45 cm between T/P&Jason-1 and 7.46 cm between Jason-1/Jason-2. An exhaustive overview over possible errors impacting the MSL evolution is given in [3].
Furthermore, annual and semi-annual signals are removed from the time serie and a 2-month filter is applied. For more details, see MSL Aviso Website : http://www.aviso.oceanobs.com/msl.

## 6.2.  Regional MSL trends

Though mean sea level trend is globally positive, it is inhomogeneous distributed over the ocean. Locally, sea level rise or decline up to $\pm 10$ mm/yr are observed on right panel of figure 23. The map of regional MSL trends is estimated from multi-mission grids (Ssalto/DUACS products) in order to improve spatial resolution. Data from Jason-2 mission were introduced in DUACS system end of January 2009 (when Jason-1 moved to its new interleaved orbit).
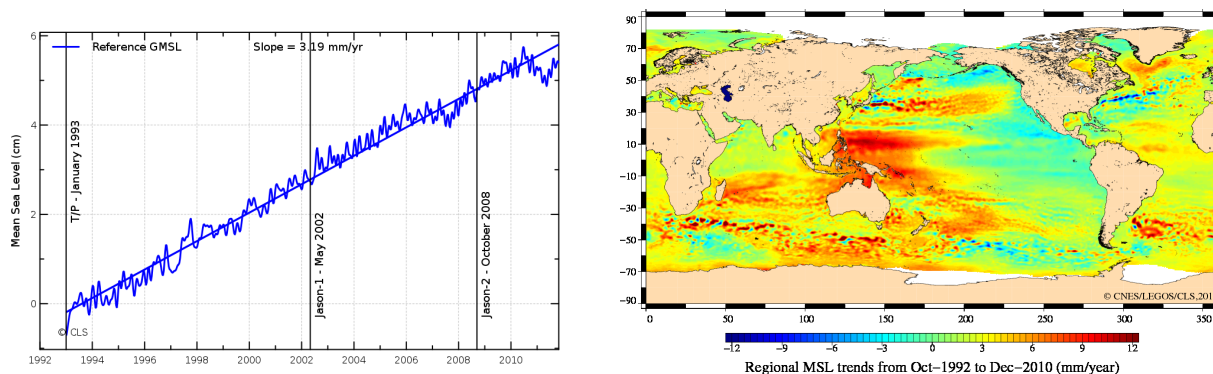


FIG. 23 – *Global (left) and regional (right) MSL trends from 1993 onwards.*

# Références

[1] Jason-2 Version 'T' Geophysical Data Records : Public Release, August 2009. Available at : http://www.aviso.oceanobs.com/fileadmin/documents/data/products/Jason-2_GDR_T_disclaimer.pdf

[2] OSTM/Jason-2 User Handbook, August 2009 *SALP-MU-M-OP-15815-CN*. Available at : http://www.aviso.oceanobs.com/fileadmin/documents/data/tools/hdbk_j2.pdf

[3] M. Ablain, Cazenave, A., Valladeau, G., and Guinehut, S. 2009 : A new assessment of the error budget of global mean sea level rate estimated by satellite altimetry over 1993-2008. *Ocean Sci,* **5,** 193-201. Available at http://www.ocean-sci.net/5/193/2009/os-5-193-2009.pdf

[4] S. Brown, S. Desai, W. Lu, and A. Sibthorpe. 2009 : Performance assessment of the Advanced Micro-wave radiometer after 1 year in Orbit. *OSTST Seattle, USA,*. Available at : http://www.aviso.oceanobs.com/fileadmin/documents/OSTST/2009/oral/Brown.pdf

[5] J.-D. Desjonqueres, G. Carayon, J.-L. Courriere, and N. Steunou, 2008. Poseidon 3 In-flight re-sults. *OSTST Nice, France*. Available at : http://www.aviso.oceanobs.com/fileadmin/documents/OSTST/2008/oral/desjonqueres.pdf

[6] J.-D. Desjonqueres, 2009. Poseidon 3 Instrument Investigations, Corrections and Upgrades. *OSTST Seattle, USA*. Available at : http://www.aviso.oceanobs.com/fileadmin/documents/OSTST/2009/oral/Desjonqueres_instrument.pdf

[7] J. Dorandeu, M. Ablain, Y. Faugere, F. Mertz & B. Soussi, 2004 : Jason-1 global statistical evalua-tion and performance assessment. Calibration and cross-calibration results. *Marine GEODESY,***27,** 345-372. See : http://www.informaworld.com/smpp/content~db=all~content=a718993059

[8] P. Thibaut et al. : Poseidon-3 Quality Assessment Report Cycle 121. SALP-RP-JALT-EX-21599-CLS-121.